JACS
JOURNAL OF THE AMERICAN CHEMICAL SOCIETY

ARTICLE

pubs.acs.org/JACS

Copper Binding Agents Acting as Copper Ionophores Lead to Caspase Inhibition and Paraptotic Cell Death in Human Cancer Cells

Saverio Tardito,[†] Irene Bassanetti,[‡] Chiara Bignardi,[‡] Lisa Elviri,[‡] Matteo Tegoni,[‡] Claudio Mucchino,[‡] Ovidio Bussolati,[†] Renata Franchi-Gazzola,[†] and Luciano Marchiò*[,‡]

[†]Dipartimento di Medicina Sperimentale, Sezione di Patologia Generale e Clinica, Via Volturno 39, 43100 Parma, Italy

[‡]Dipartimento di Chimica Generale ed Inorganica, Chimica Analitica, Chimica Fisica, Università degli Studi di Parma, Viale G.P. Usberti 17/A, 43100 Parma, Italy

Supporting Information

ABSTRACT: We report a quantitative structure−activity relationship study of a new class of pyrazole-pyridine copper complexes that establishes a clear correlation between the ability to promote copper accumulation and cytotoxicity. Intracellular metal accumulation is maximized when ligand lipophilicity allows the complex to rapidly cross the membrane. Copper and ligand follow different uptake kinetics and reach different intracellular equilibrium concentrations. These results support a model in which the ligand acts as an ionophore for the metal ion, cycling between intra- and extracellular compartments as dissociated or complexed entities. When treating cancer cells with structurally unrelated disulfiram and pyrazole-pyridine copper complexes, as well as with inorganic copper, the same morphological and molecular changes were reproduced, indicating that copper overload is responsible for the cytotoxic effects. Copper-based treatments drive sensitive cancer cells toward paraptotic cell death, a process hallmarked by endoplasmic reticulum stress and massive vacuolization in the absence of apoptotic features. A lack of caspase activation, as observed in copper-treated dying cells, is a consequence of metal-mediated inhibition of caspase-3. Thus, copper acts simultaneously as an endoplasmic reticulum (ER) stress inducer and a caspase-3 inhibitor, forcing the cell into caspase-independent paraptotic death. The establishment of a mechanism of action common to different copper binding agents provides a rationale for the exploitation of copper toxicity as an anticancer tool.

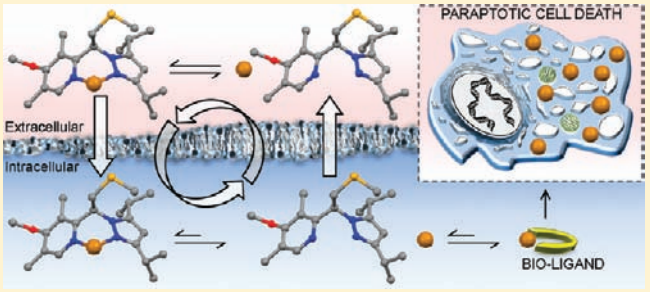

INTRODUCTION

The use of metal ions in medicine can be traced back to the early stages of civilization. Their (multi)positive charges and stereoelectronic properties make them particularly apt to alter the structure and function of important biological targets. As such, metal ions are fundamental components of the biochemical machinery. Notably, 47% of enzymes contain metals (41% in their catalytic centers).[1] For this reason, the transport and homeostasis of metal ions are strictly controlled with specific chaperones that have been evolutionarily designed.

Metal complexes have been investigated in recent decades as potential anticancer compounds, largely due to the success of cisplatin. This compound, one of the most widely employed chemotherapeutic agents, has had a major impact on the treatment of several tumor types, especially for testicular and ovarian cancers.[2] The efforts of synthetic chemistry to provide novel anticancer agents have focused on low-toxicity platinum-based and nonplatinum-based drugs with alternative mechanisms of action. Regarding the latter, ruthenium,[3] gold,[4] and titanium[5] have been investigated as candidates for the production of anticancer compounds. In all of these cases, ligands that are able to modulate metal ion reactivity and toxicity may contribute to a successful outcome.

Copper is a fundamental component of metalloproteins because it exerts both catalytic and structural functions and its distribution is strictly regulated at the levels of the cell, organ, and body.[6−8] Mutations in the genes coding for the copper transporters ATP7A and ATP7B impair copper handling and result in Menkes and Wilson diseases, respectively.[9] Copper also plays important roles in neoplastic diseases.[10] In particular, copper is crucial to the angiogenic process that sustains tumor and metastasis development, and its sequestration underlies an anticancer strategy aimed at preventing establishment of the tumor blood supply.[11] Alternatively, copper complexes have shown anticancer activity, whereby the organic component (the ligand) is responsible for directing the metal to different molecular targets.[12]

Although the majority of anticancer compounds trigger apoptosis, other types of programmed cell death (PCD) occur in response to common treatment regimens.[13,14] Among the

Received: November 2, 2010
Published: March 31, 2011

Scheme 1. Synthesis of Pyrazole-Pyridine Ligands L1−L10

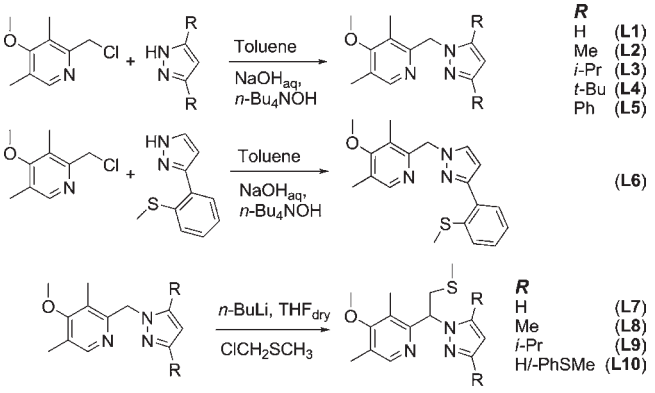

Scheme 2. Synthesis of Bispyrazole Ligands L11−L20

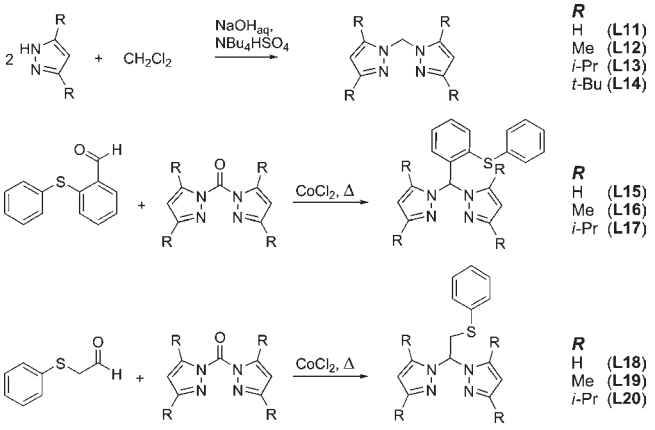

various types of PCD, paraptosis, characterized by the occurrence of large cytoplasmic vacuoles derived from the endoplasmic reticulum (ER),[15] was observed in cancer cells treated with different copper complexes.[16,17] A comparison between the transcriptional responses elicited by cisplatin or a thioxotriazole copper complex, showed activation of distinct pathways.[18] Whereas cisplatin triggers canonical p53-dependent apoptosis, the copper complex causes irreversible ER stress, ER vacuolization and, eventually, paraptotic cell death.

To understand the structural basis of these effects, we prepared and screened a series of pyrazole-pyridine and bis-pyrazole copper complexes for cytotoxicity. The effects of the most active compound were compared with those of inorganic copper and disulfiram, a copper-interacting drug with promising anticancer properties.[19] The results showed that (a) the copper complexes induce paraptosis as a function of their ability to cause intracellular copper accumulation, (b) the metal itself is sufficient to produce paraptotic features in cancer cells (provided that high doses are used), and (c) during copper-dependent lethal ER stress, caspase-3 inhibition by the metal accounts for the switch from apoptotic to paraptotic cell death.

RESULTS

Structure−activity Relationship of Novel Cytotoxic Copper Complexes. To establish a relationship between the structure of the ligand fragment and the cytotoxic activity of the resulting Cu(II) complexes, specific structural modifications were applied to bis-pyrazole and pyrazole-pyridine, two molecular backbones endowed with N,N copper-coordinating abilities. The synthesis of the pyrazole-pyridine derivatives is described in Scheme 1. Ligands **L1**−**L6** were prepared by reacting the electrophilic chloroethyl-dimethylpyridine and pyrazole, in biphasic solvent (toluene/water) via phase transfer catalysis (*n*-Bu$_4$NOH).[20] The preparation of **L7**−**L10** ligands is preformed by treating the pyrazole-pyridine parent compounds with *n*-BuLi and an electrophile bearing a thioether function (ClCH$_2$SCH$_3$).[21,22]

The bis-pyrazole ligands **L11**−**L14** were prepared by refluxing deprotonated pyrazoles in dichloromethane, whereas ligands **L15**−**L20** were prepared by treating bis(pyrazolyl)ketones with aldehydes bearing the desired sulfur donor groups that were to be attached to the bispyrazole scaffold (Scheme 2).[23−25]

Copper complexes were then prepared by mixing equimolar amount of CuCl$_2$·2H$_2$O and **L1**−**L20** ligands in methanol. In most of the cases, the product precipitated out from the green solution, from which it was recovered.

According to the molecular backbone and the nature of a thioether third arm on the carbon center linking the two rings, the ligands could be divided into five classes (**a**−**e**, Figure 1).

Within each class, peripheral residues on the pyrazole ring were modified to vary the hydrophobicities or coordinative abilities of ligands. Specifically, hydrophobicity was modulated by substituting the H-atom of the parent compound with Me and *i*-Pr as well as *t*-Bu and Ph when synthetically feasible. To influence coordinative ability, a thioether group was introduced on the pyrazole ring of compounds **6** and **10**. According to the X-ray structures reported in Figure 2 and in the Supporting Information, the invariant feature of the Cu(II) complexes is an *N*,*N*-chelation motif, whereas sulfur binding strongly depends on the types of thioether fragments introduced. In fact, the sulfur atom participates in metal coordination only when it is introduced in a favorable steric position (compounds **6** and **10**, Figures 1 and 2). When the thioether was attached as a flexible (compounds **7**−**9** and **18**−**20**) or rigid (**15**−**17**) central arm, it influenced the hydrophobicity of the ligand, but not its coordinative properties. The molecular structures can be grouped in two categories: mononuclear and dinuclear. In the first case, the metal geometry is flattened tetrahedral (compounds **4**, **5**, **13**, **17**, **19**, and **20**), whereas for the dinuclear case, the metal geometry is square pyramidal, with the apex of the pyramid occupied by a bridging chloride anion (compounds **2**, **3**, **7**, **8**, **9**, **15**, and **16**). Exceptions are represented by compounds **6** and **10** that exhibit a trigonal bypyramidal geometry by virtue of the presence of the N, N,S ligand donor set, and by compound **11** that forms chains constituted by the tetrahedral $[CuCl_4]^{2-}$ anion and the octahedral $[Cu(\mathbf{L11})_2]^{2+}$ cation. Crystals suitable for X-ray data collection could not be obtained for compounds **1**, **12**, **14**, and **18**. Nevertheless, on the basis of the molecular structures of homologous compounds, it may be expected that the ligands behave as N,N donors, **1**/**18** present dinuclear structures, whereas compounds **12** and **14** exhibit mononuclear structures. This tentative hypothesis can be justified by the presence or absence of steric hindrance on the pyrazole rings of compounds **1**/**18** and **12**/**14**, respectively.

The anticancer activities of the complexes were evaluated in human fibrosarcoma HT1080 cells by means of a resazurin-based viability assay. Given that some compounds exhibited dinuclear structures and some others mononuclear structures, the dose

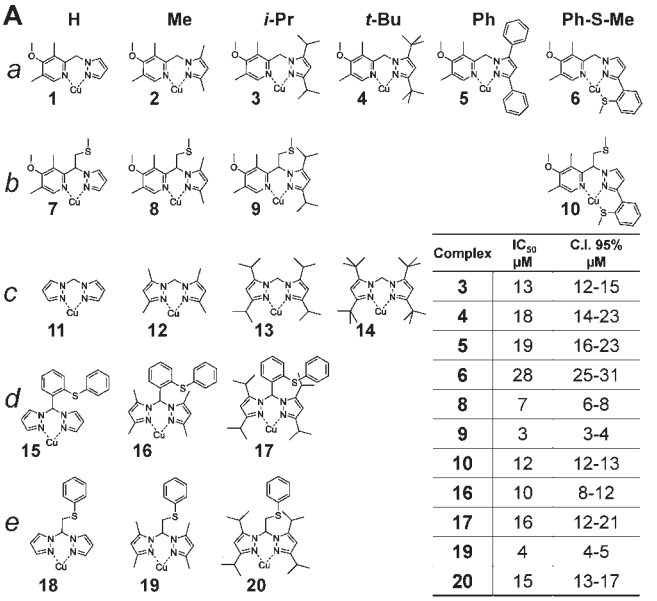

Complex	IC_{50} μM	C.I. 95% μM
3	13	12-15
4	18	14-23
5	19	16-23
6	28	25-31
8	7	6-8
9	3	3-4
10	12	12-13
16	10	8-12
17	16	12-21
19	4	4-5
20	15	13-17

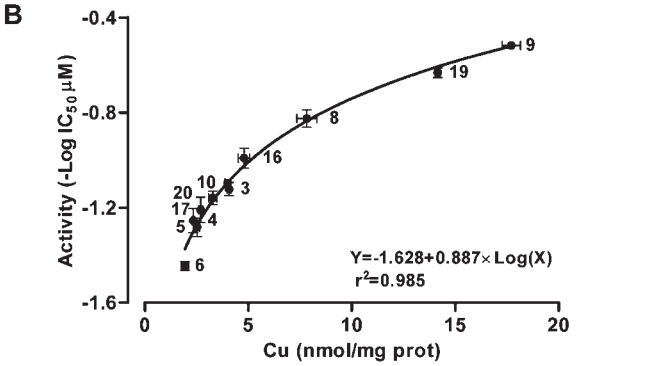

Figure 1. (A) Pyrazole-pyridine-based (rows *a*, *b*) and bis-pyrazole-based (rows *c*, *d*, and *e*) copper(II) complexes. The coordinated chloride anions are omitted for clarity. The table shows IC_{50} values for complexes that are able to decrease HT1080 cell viability by more than 50% with respect to the control. C.I. 95%: confidence interval at 95% for the IC_{50} values. Cells were treated with complexes in the 1−30 μM range for 48 h. (B) Relationship between cytotoxic activity and the cellular copper concentration obtained by treating HT1080 cells for 6 h with 13.2 μM of the indicated complexes. Cellular copper concentration was determined by ICP-AES. The points are means ± SEM of three independent experiments, with six and two replicates for viability and copper determination, respectively.

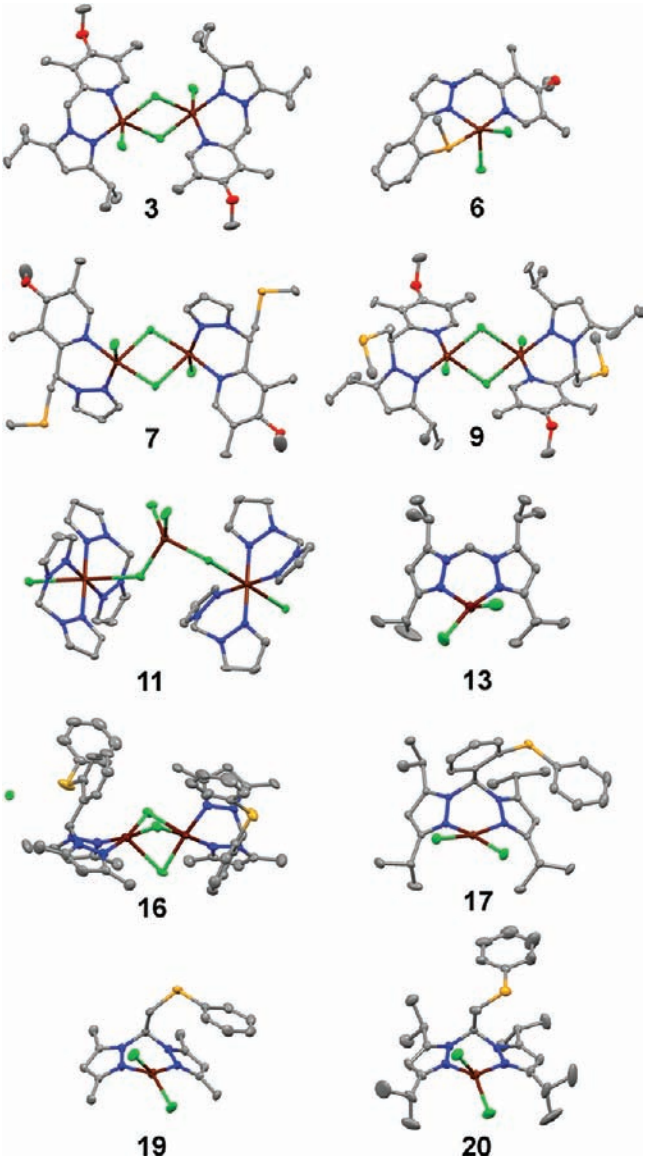

Figure 2. X-ray molecular structures of representative Cu(II) complexes. Solid thermal ellipsoids are reported at the 30% probability level. Hydrogen atoms are omitted for clarity: C (gray), N (blue), Cl (green), O (red), S (yellow), Cu (brown).

response curves were based on the concentration of copper ion. The IC_{50} values (Figure 1A), extrapolated from the dose response curves reported in Supporting Information Figure S8, allowed us to identify the following structure−activity relationships: (i) substitution of the H-atom on the pyrazole ring is essential for the activity of the complex and (ii) both the presence of the pyridine in place of pyrazole (compare classes **a** with **c**) and the presence of the central thioether arm (compare classes **a** with **b** and **c** with **d** and **e**) enhance activity. The highest activity was observed for classes with flexible thioether groups (compare classes **b** with **d** and **e**). Among the 20 compounds, **9** was the most active (IC_{50} = 3 μM). The rank of the IC_{50} values within each class points to the fundamental role of ligand hydrophobicity in the biological response of the corresponding Cu(II) complex. The relationship between the calculated logP value[26] of the ligand and the cytotoxic activity of the respective complex suggests that, for each class of compounds, there is an optimal logP value (between 4 and 6) at which activity is maximal (Supporting Information Figure S9).

The stability of the Cu(II)-ligand complexes was assessed by evaluating the equilibrium formation constant as derived from the following equation: Cu(II) + L ⇌ Cu(II)L (β = [Cu(II)L]/([Cu(II)]·[L])). The logβ value was determined for five complexes; it varied between 3.34 ± 0.15 and 4.69 ± 0.08 (Supporting Information Figure S7A). As expected, the highest stability was found for compound **10**, which employs three donor atoms (N,N,S) for copper binding instead of the bidentate N,N coordination seen in all of the other complexes. Higher stability was not associated with increased cytotoxicity. Speciation calculations (Supporting Information Figure S7B) showed that, when

dx.doi.org/10.1021/ja109413c |*J. Am. Chem. Soc.* 2011, 133, 6235–6242

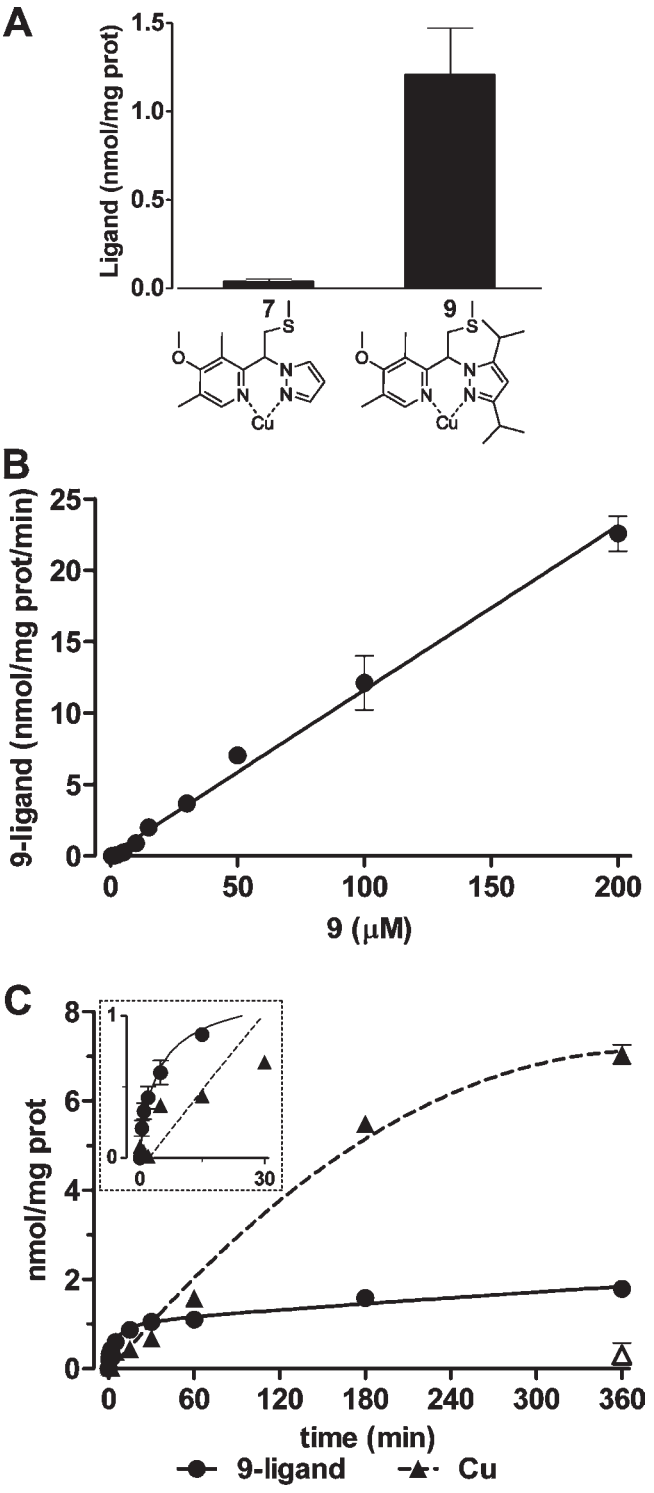

Figure 3. (A) Cellular concentrations of 7- and 9-ligands were determined by RPLC ESI-MS. HT1080 cells were incubated for 6 h with 5 μM of the indicated complexes. (B) Uptake of 9-ligand in HT1080 cells incubated for 2 min with the indicated concentrations of 9 (5−200 μM). (C) Uptake kinetics of 9-ligand (solid line) and copper (dotted line). HT1080 cells were incubated with 9 (5 μM) for the indicated time periods (0.5−360 min). The copper content of cells incubated with 5 μM $CuCl_2$ for 360 min is reported for comparison (△). The inset is an enlargement of the first 30 min of uptake. All data are means ± SEM of two independent experiments with three replicates each.

the ligand of compound 9 and copper were present at 5 μM each, the expected concentration of the complex was less than 50 nM, a value that would decrease further if copper-binding competitors were taken into account. It may then be expected that for all the complexes the metal should be largely displaced from the ligands by the copper-binding competitors present in the cell culture medium.

Cell copper content was determined for the eleven active complexes (IC_{50} < 30 μM) by means of ICP-AES. When cells were incubated with the complexes at constant concentrations corresponding to the mean IC_{50} (13.2 μM), a strong correlation emerged between cytotoxic activity and cell copper content (nonparametric Spearman r = 1). Figure 1B describes the relationship between these two parameters and indicates that the ability of a complex to promote copper accumulation in the cell depends on the ligand structure and is predictive of its cytotoxic activity.

Characterization of Ligands and Copper Uptake in Cells Treated with Pyrazole-Pyridine Copper Complexes. To correlate cytotoxic activity and complex bioavailability, we assessed ligand uptake of the most active compound 9 and of the inactive compound 7. The cell extracts were analyzed by means of Reversed-Phase Liquid Chromatography (RPLC) combined with an electrospray ionization linear ion trap (ESI-LIT) mass spectrometry. As shown in Figure 3A, the accumulation of 9-ligand was 30-fold higher than that observed for the ligand of the inactive (and less lipophilic) compound 7. This evidence strongly suggests that passive diffusion accounts for membrane crossing for this class of complexes. To verify this hypothesis, a dose-dependent uptake experiment was performed in live cells. Figure 3B shows the linear relationship between the intracellular concentration of 9-ligand and the extracellular concentration of 9. These results indicate that, in the range of concentrations tested, ligand transport is not saturated and follows the Fick law for passive diffusion. The accumulation of 9-ligand reached a plateau by approximately 30 min (Figure 3C). On the contrary, under the same experimental conditions, copper uptake showed much slower kinetics, approaching a steady state at 360 min. However, at this time, in cells incubated with 5 μM of complex 9, the intracellular copper content was approximately 4-fold higher than the intracellular ligand content and more than 20-fold higher than the copper level observed upon incubation with 5 μM inorganic copper. These results suggest that the ligand carries copper across the membrane bilayer by virtue of its lipophilicity and favors its accumulation in the intracellular compartment, acting as an ionophore for the metal.

Relationship between Copper Content and Biological Responses of Tumor and Normal Cells. Given the positive correlation between the cytotoxic activity of **1**−**20** and the cell copper content obtained with the same complexes (see Figure 1B), we investigated whether inorganic copper ($CuCl_2$) was sufficient to produce similar effects. The cytotoxic response to $CuCl_2$ was assessed in three human tumor cell lines (HT1080, HeLa, and SW872) and normal fibroblasts (HF) and compared with the effects of the most active compound 9. The dose response curve showed that $CuCl_2$ was toxic above 200 μM, while compound 9 was active at concentrations less than 10 μM (Supporting Information Figure S10A and B). When $CuCl_2$ was used at a toxic concentration, the morphological changes induced were identical to those caused by compound 9 (see Figure 5A). These alterations were similar to those described for a thioxotriazole copper(II) complex that induces paraptosis.[16,18] The correlation between cell copper accumulation and cytotoxicity

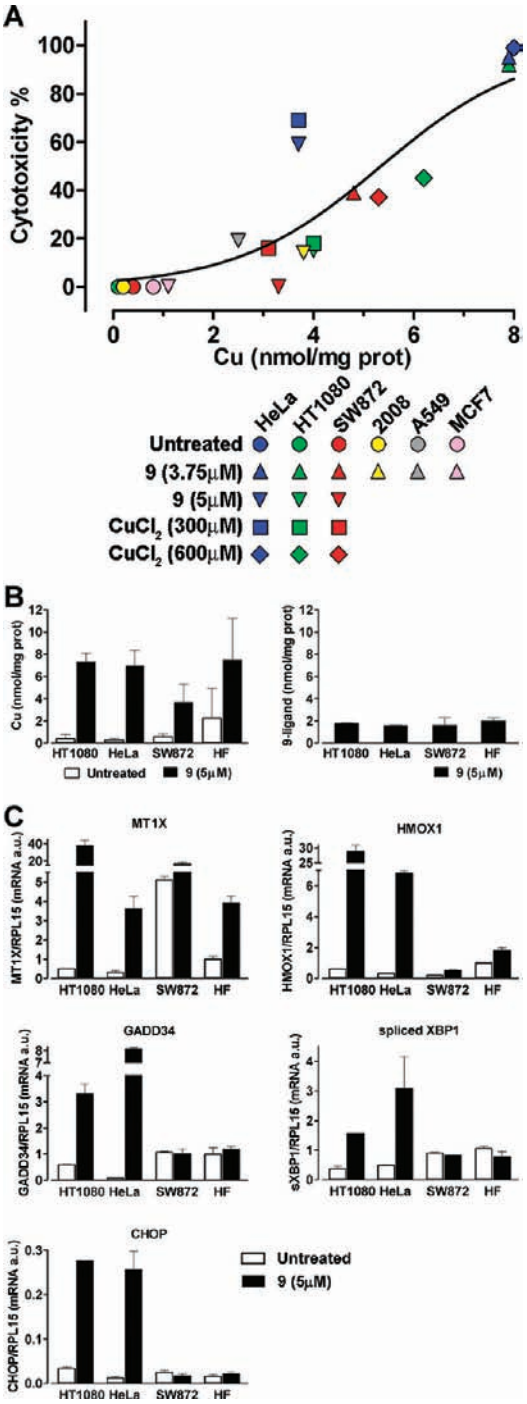

Figure 4. (A) Tumor cell lines were treated with compound **9** or $CuCl_2$ at the indicated concentrations for 6 h. Untreated cells were used as the control. Cytotoxicity (48 h) is plotted vs cell copper content (6 h), and the data are fitted with a nonlinear regression curve ($r^2 = 0.8$). Data are means of three determinations of a representative experiment. (B, left) Cell content of copper (ICP-AES). (right) Cell content of **9**-ligand (RPLC ESI-MS). Cells were incubated for 6 h with 5 μM of **9**. Data are means ± SD of three independent experiments with three replicates each. (C) qPCR analysis of gene expression induced by **9**. Cells were left untreated (white bars) or incubated for 9 h with 5 μM of **9** (black bars). The expression levels of the indicated genes are normalized for the amount of RPL15 mRNA and are reported as arbitrary units. Data are means ± SD of two independent experiments with three replicates each.

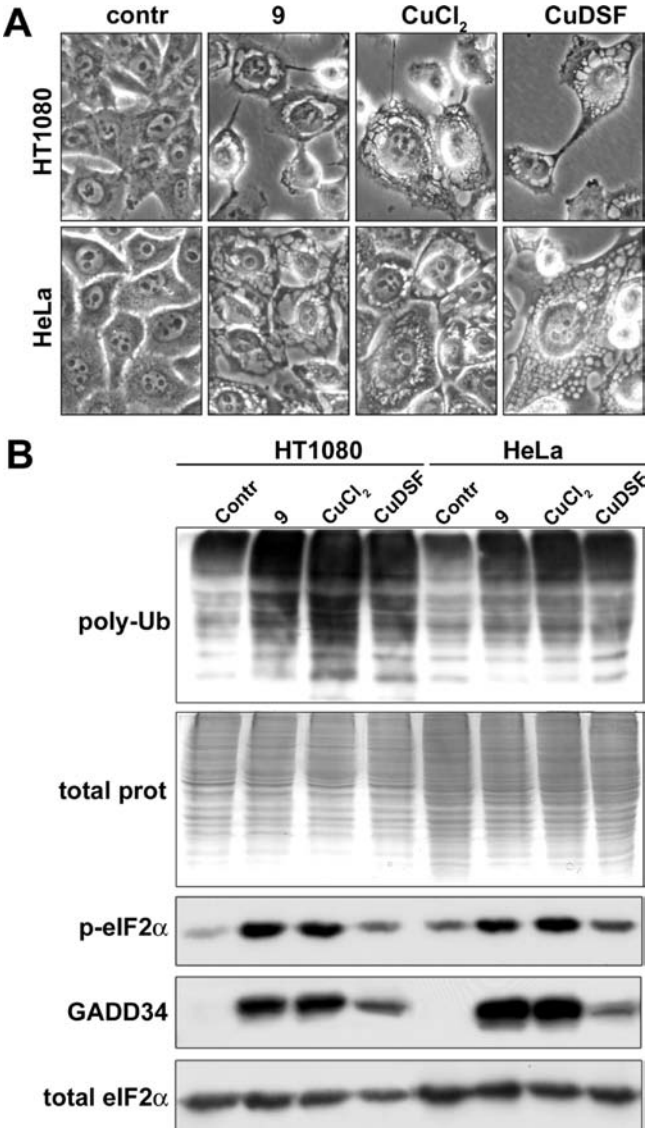

Figure 5. (A) Phase contrast images representative of HT1080 or HeLa cells incubated for 15 h with **9** (5 μM), $CuCl_2$ (750 μM), or CuDSF (1.5 μM). Vacuolated cells are evident in treated cultures (original magnification: 400×). (B) Immunoblot analysis of UPR markers. HT1080 and HeLa cells were treated as in A, and extracts were analyzed to detect polyubiquitinylated proteins (poly-Ub), eIF2α phosphorylated in S51 (p-eIF2α), and GADD34. Ponceau staining of the poly-Ub blotted membrane (total prot) and total eIF2α are shown as the loading control.

induced by the various complexes (Figure 1B) holds true for compound **9** and $CuCl_2$ in HT1080, HeLa, SW872 2008, A549, and MCF7 cells (nonparametric Spearman $r = 0.86$, Figure 4A). Therefore, copper itself appears to be responsible for the biological alterations induced in tumor cell lines, independently of cancer cell type and of the presence of the ligand. An exception was represented by normal human fibroblasts (HF), where high intracellular copper concentration did not translate into cytotoxicity, as should be expected from the curve in Figure 4A. The results obtained in HF treated with complex **9** (Figure 4B and Supporting Information Figure S10) prove that these cells are able to withstand an intracellular copper concentration (7.5 nmol/mg prot) that is toxic for cancer cells. Notably, when

dx.doi.org/10.1021/ja109413c |J. Am. Chem. Soc. 2011, 133, 6235–6242

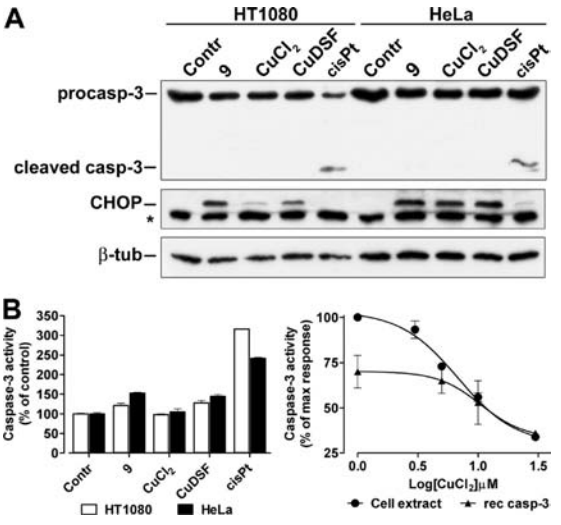

Figure 6. (A) Immunoblot analysis of caspase-3 and CHOP. HT1080 and HeLa cells were treated for 15 h with **9** (5 μM), $CuCl_2$ (750 μM), CuDSF (1.5 μM), or cisplatin (cisPt, 20 μM) and extracts were analyzed to detect both the inactive (procasp-3) and active (cleaved casp-3) forms of caspase-3. The same membrane was blotted for the ER stress-related, pro-death protein CHOP. The * symbols corresponds to a nonspecific band. β-Tubulin is shown as a loading control, and cisplatin (cisPt) is used as a positive control for apoptosis. (B) Effects of inorganic or complexed copper on caspase-3 activity. (left) Cell extracts used for the immunoblots shown in A analyzed for caspase-3 activity. Data are means $\pm$ SD of six replicates of a representative experiment. (right) HT1080 cells treated with cisplatin as in A. Cell extracts (circles) or a solution of purified human recombinant caspase-3 (triangles) were incubated for 1 h with $CuCl_2$ (1−30 μM) and then analyzed for caspase-3 activity. The results are reported as the percentage of the maximal activity obtained in the absence of $CuCl_2$. Data are means $\pm$ SD of three independent experiments with three replicates each.

HT1080, HeLa, SW872, and HF were treated for 6 h with 5 μM of compound **9**, cell copper contents were not related to the cell contents of **9**-ligand (Figure 4B). In fact, copper always reached significantly higher cell levels than the ligand, with a copper/ligand ratio that varied from 2.3 to 4.4. These results confirm that ligand and copper establish different transmembrane gradients.

To verify if the paraptotic "transcriptional fingerprint" induced in HT1080 cells by a cytotoxic thioxotriazole copper(II) complex[18] was reproduced by complex **9**, we assessed the expression of markers involved in metal-induced response (MT1X), oxidative stress (HMOX), and endoplasmic reticulum (ER) stress (CHOP, GADD34, sXBP1) experiments. In HT1080 cells, compound **9** markedly induced all tested genes (Figure 4C), confirming that copper complexes with unrelated ligand structures induce the same molecular events associated with paraptosis. The ability of compound **9** to induce this transcriptional response in other cell models was evaluated. As expected, MT1X mRNA was increased as a result of an increase in cellular copper concentration in all cell types tested. On the contrary, the induction of HMOX, a known indicator of oxidative stress[27] was considerably higher in the two sensitive cell lines (48- and 23-fold induction, normalized to the control value, for HT1080 and HeLa cells, respectively) compared to the less sensitive SW872 and HF cells (2.5- and 1.8-fold induction, respectively). The genes encoding ER stress executors were upregulated exclusively in the sensitive HT1080 and HeLa cells.

Promotion of Massive Cytoplasmic Vacuolization and the Unfolded Protein Response by Inorganic and Complexed Copper. The anticancer activity of disulfiram (DSF), an inhibitor of aldehyde dehydrogenase used in ethilism therapy, is markedly enhanced by copper[28,29] and a clinical trial with DSF in combination with copper against liver cancer is in the recruitment phase (ClinicalTrials.gov Identifier: NCT00742911). When equimolar amounts of $CuCl_2$ and DSF were administered to HT1080 and HeLa cells (Figure 5A), massive cytoplasmic vacuolization in the absence of apoptotic features was observed. These morphological changes coincided with the paraptotic morphology[15,16] caused by complex **9** or $CuCl_2$ and observed with [Cu(8-hydroxiquinoline)$_2$] and [Cu(clioquinole)$_2$], which promote copper transport into cells[30] (Supporting Information Figure S11). Consistent with previous data,[28,29,31,32] the metal shifted the IC_{50} value of DSF from 5.2 to 0.4 μM and from 15.7 to 0.4 μM in HT1080 and HeLa cells, respectively.

ER-derived paraptotic vacuolization is part of the unfolded protein response (UPR) that is sustained by unresolved ER stress.[18,33] Consistently, in HT1080 and HeLa cells, complex **9**, $CuCl_2$, and CuDSF all increased the amount of polyubiquitinylated proteins, the causal event of the UPR (Figure 5B). Moreover, in both cell models, complex **9**, $CuCl_2$, and CuDSF increased the ratio between phosphorylated and total eukaryotic initiation factor 2 alpha (eIF2α), the phosphorylation of which promotes the UPR.[34] GADD34, an ATF4-dependent UPR target gene downstream of eIF2α, was barely detectable in untreated cells but was clearly induced in both cell lines treated with compound **9**, $CuCl_2$, or CuDSF.

Caspase Inhibition by Inorganic and Complexed Copper. The activation of caspases, the apoptotic execution machinery, was assessed during treatment with inorganic ($CuCl_2$) or complexed copper (**9** and CuDSF). Supporting Information Figure S12A shows images of HT1080 cultures undergoing cell death upon treatment with cisplatin, complex **9**, $CuCl_2$, or CuDSF. In a significant fraction of cells, cisplatin clearly induced an apoptotic morphology, including nuclear fragmentation (DAPI staining) and caspase activation, as visualized with a fluorogenic pan-caspase substrate. On the contrary, vacuolated cells, treated with either inorganic or complexed copper, were negative for caspase and exhibited neither chromatin condensation nor nuclear fragmentation in apoptotic bodies. In both HT1080 and HeLa cells, differential caspase-3 behavior in cisplatin-treated and copper-treated cells was confirmed by Western blot, with the cleaved form much more evident in cisplatin-treated than in copper-treated cells (Figure 6A), where caspase activation was only detectable after prolonged film exposure (Supporting Information Figure S12B). The expression of a known pro-death ER stress-related protein, CHOP, was clearly induced by all of the copper-based treatments, whereas it remained undetectable or slightly induced in cisplatin treated HT1080 and HeLa cells, respectively (Figures 6A and Supporting Information Figure S12B).

The activity of caspase-3 was also evaluated in extracts of cells incubated with complex **9**, $CuCl_2$, CuDSF, or cisplatin (Figure 6B). Copper-based compounds increased caspase activity by 21% and 53% in HT1080 and HeLa cells, respectively, whereas cisplatin induced increases of 216% and 142%, respectively.

The effects of copper ($CuCl_2$) on caspase-3 activity were directly assessed in either extracts of HT1080 cells pretreated with cisplatin or human recombinant caspase-3 in solution

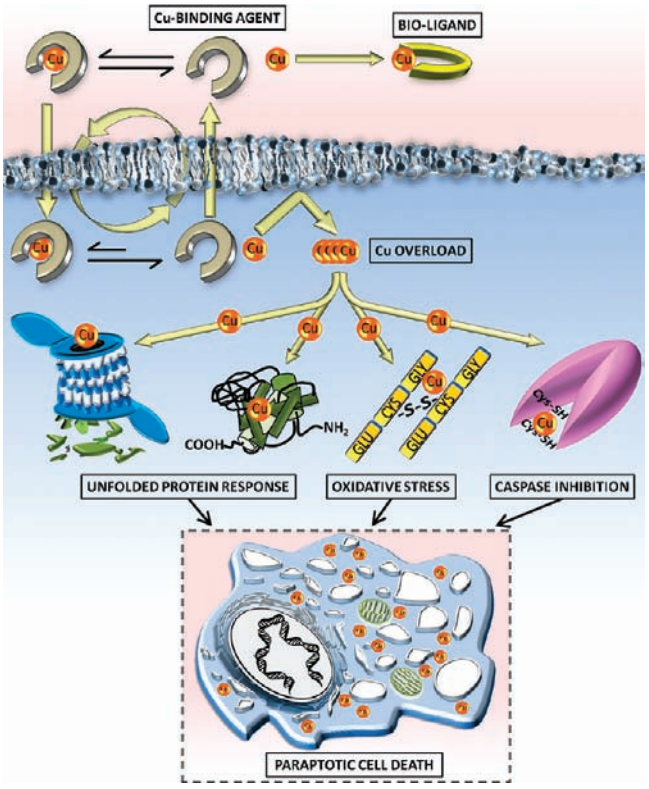

Figure 7. Proposed model for a copper-binding agent mechanism of action.

(Figure 6B). The two dose−response curves show that copper inhibits caspase with an IC_{50} of 11.5 μM and a maximum inhibition of 70% at 30 μM. Nevertheless, the two responses are distinct, as only the activity of recombinant caspase-3 was significantly inhibited at 1 μM $CuCl_2$.

DISCUSSION

This study demonstrates that lipophilicity is a relevant determinant of the cytotoxic activity of a copper complex. The highest activity is reached with an optimal ligand hydrophobicity that allows rapid equilibrium of the complex between the lipid (cell membranes) and aqueous compartments (intra- and extracellular). For lower logP values, the Cu(II)-ligand ensemble may be too hydrophilic to cross the cell membrane efficiently, while for higher logP values, the complex may prefer to stay in the membrane fraction. Thus, ligands contribute to copper toxicity by facilitating metal release into the cell, according to the mechanism of action model proposed in Figure 7. However, the fact that the correlation between logP value and cytotoxicity does not obey the same law for the five ligand classes (Supporting Information Figure S9) indicates that other parameters influence cytotoxic activity.

According to the stability constant, the ligand is mostly dissociated from the metal in the extracellular environment, where copper is sequestered by binding to competitors such as amino acids and serum proteins. For instance, the stability of the [Cu(histidine)$_2$] complex is several orders of magnitude higher than the stabilities of the complexes studied here.[12] Nevertheless, the portion of copper that remains complexed, following the diffusion law, equilibrates between the extracellular and intracellular spaces. It is worth mentioning that, despite its high stability, the [Cu(histidine)$_2$] complex exhibits negligible cytotoxic activity (Supporting Information Figure S11).

In the cell, high concentrations of high-affinity Cu-binding proteins and ligands are present (i.e., glutathione may reach concentrations of approximately 10 mM), entrapping the metal, which cannot freely pass the plasma membrane; conversely, neutral ligands with optimal lipophilicity (such as that of complex **9**) freely move across the three compartments. The kinetics of complex dissociation may also play a role in influencing the amount of complex that can cross the membrane. Steric encumbrance at the metal center, as seen for ligands with a mobile thioether group, can slow substitution kinetics by hindering the interaction with potential biological chelators. This fact may explain why complexes **9** and **19** are more active than complexes **3** and **16**. Provided that it is used at sufficiently high concentrations, inorganic copper causes the same effects observed for copper complexes, thus yielding further evidence that the complex is dissociated inside cells.

This study demonstrates that there is a correlation between observed cytotoxicity and the intracellular copper content. How can high levels of intracellular copper cause cytotoxicity? Given that no free copper ions are available inside eukaryotic cells,[35] the metal is largely coordinated by reduced glutathione (GSH), the major redox buffer system of the cell, hence perturbing the GSH/GSSG ratio.[36,37] Because correct protein folding needs a controlled redox environment, a lack of copper-dependent oxidative balance can markedly affect protein conformation.[38] Furthermore, when the copper-handling capacity of the cell is exceeded, the metal binds to nonspecific targets and may perturb their structure and function, as is the case of copper-induced proteasome inhibition that leads to the accumulation of misfolded proteins.[18,31,39] These combined events cause unsolvable ER stress, manifested as massive cytoplasmic vacuolization, and activation of the UPR (eIF2α phosphorylation, XBP1 splicing, induction of GADD34 and CHOP).[34] Therefore, a different response to misfolded protein accumulation and ER stress (i.e., eIF2α phosphorylation) may translate into different sensitivities to copper overload, explaining the variability observed between the cell models used in this study.

Although UPR may link ER stress to the apoptotic pathway through the induction of pro-death proteins such as CHOP, apoptosis is not observed in the death process triggered by high intracellular copper levels because the metal itself inhibits caspase-3. Despite the lack of evidence for a direct interaction with the enzyme, it is likely that copper interferes with catalytic cysteine residues in the active site. The different inhibition profiles of caspase-3, obtained with purified recombinant enzyme or cell lysates, may be reasonably explained by taking into account the presence of several metal-binding species in crude extracts that impair the copper-caspase interaction. This phenomenon was previously described in a study that assessed the role of Zn(II) in caspase inhibition.[40]

Our findings point to a mechanism of action for copper binding agents that can also apply to disulfiram (DSF), a copper-interacting drug repeatedly described as an apoptotic inducer in several in vitro and in vivo cancer models.[31,32] In our models, DSF concentrates copper in the cell (Supporting Information Figure S11B), reproducing the morphological and molecular changes observed with other copper complexes, indicative of paraptotic cell death (Figures 5 and 6). Only in a very limited fraction of treated cells CuDSF causes apoptotic

changes, which is consistent with the marginal increase in the caspase-3 activity observed under these conditions.

For the copper complexes examined in this study, as well as for other previously described compounds,[17,37] the biological effects consistently observed are the intracellular accumulation of high amounts of copper, the appearance of cytoplasmic vacuolization, and the activation of caspase-independent cell death. These observations can be reasonably explained if the ligand behaves as a copper ionophore that exacerbates the intrinsic toxicity of the metal by increasing its intracellular concentration. If a ligand has autonomous biological activities, as in the case of DSF, the two effects might be synergistic, leading to a potent cytotoxic behavior. Since DSF associated with copper is currently under clinical investigation as an anticancer agent, these findings may be useful for designing an effective therapeutic combination with pro-apoptotic drugs.

■ ASSOCIATED CONTENT

Supporting Information. Synthesis of ligands and copper complexes, stability constants determination, X-ray structures of **2**−**9**, **11**−**13**, **15**−**17**, and **19**−**20** complexes (CCDC 792828−792842), cell cultures, Western blots, cell viability assays, real time PCR, copper and ligand cellular uptake assays, caspase-3 activity assays, and supporting figures. This material is available free of charge via the Internet at http://pubs.acs.org.

■ AUTHOR INFORMATION

Corresponding Author
marchio@unipr.it

■ ACKNOWLEDGMENT

This work has been funded by a MIUR grant to L.M. (PRIN 2007 20078EWK9B_003).

■ REFERENCES

(1) Guengerich, F. P. *J. Biol. Chem.* **2009**, *284*, 709.
(2) Kelland, L. *Nat. Rev. Cancer* **2007**, *7*, 573.
(3) Antonarakis, E. S.; Emadi, A. *Cancer Chemother. Pharmacol.* **2010**, *66*, 1.
(4) Nobili, S.; Mini, E.; Landini, I.; Gabbiani, C.; Casini, A.; Messori, L. *Med. Res. Rev.* **2010**, *30*, 550.
(5) Kostova, I. *Anticancer Agents Med. Chem.* **2009**, *9*, 827.
(6) Kim, B. E.; Turski, M. L.; Nose, Y.; Casad, M.; Rockman, H. A.; Thiele, D. J. *Cell Metab.* **2010**, *11*, 353.
(7) Banci, L.; Bertini, I.; Ciofi-Baffoni, S.; Kozyreva, T.; Zovo, K.; Palumaa, P. *Nature* **2010**, *465*, 645.
(8) Collins, J. F.; Prohaska, J. R.; Knutson, M. D. *Nutr. Rev.* **2010**, *68*, 133.
(9) de Bie, P.; Muller, P.; Wijmenga, C.; Klomp, L. W. J. *J. Med. Genet.* **2007**, *44*, 673.
(10) Turski, M. L.; Thiele, D. J. *J. Biol. Chem.* **2009**, *284*, 717.
(11) Finney, L.; Vogt, S.; Fukai, T.; Glesne, D. *Clin. Exp. Pharmacol. Physiol.* **2009**, *36*, 88.
(12) Tardito, S.; Marchiò, L. *Curr. Med. Chem.* **2009**, *16*, 1325.
(13) Broker, L. E.; Kruyt, F. A. E.; Giaccone, G. *Clin. Cancer Res.* **2005**, *11*, 3155.
(14) Brown, J. M.; Attardi, L. D. *Nat. Rev. Cancer* **2005**, *5*, 231.
(15) Sperandio, S.; de Belle, I.; Bredesen, D. E. *Proc. Natl. Acad. Sci. U.S.A.* **2000**, *97*, 14376.
(16) Tardito, S.; Bussolati, O.; Gaccioli, F.; Gatti, R.; Guizzardi, S.; Uggeri, J.; Marchiò, L.; Lanfranchi, M.; Franchi-Gazzola, R. *Histochem. Cell Biol.* **2006**, *126*, 473.
(17) Marzano, C.; Pellei, M.; Colavito, D.; Alidori, S.; Gioia-Lobbia, G.; Gandin, V.; Tisato, F.; Santini, C. *J. Med. Chem.* **2006**, *49*, 7317.
(18) Tardito, S.; Isella, C.; Medico, E.; Marchiò, L.; Bevilacqua, E.; Hatzoglou, M.; Bussolati, O.; Franchi-Gazzola, R. *J. Biol. Chem.* **2009**, *284*, 24306.
(19) Cvek, B.; Dvorak, Z. *Drug Discov. Today* **2008**, *13*, 716.
(20) Gennari, M.; Tegoni, M.; Lanfranchi, M.; Pellinghelli, M. A.; Marchiò, L. *Inorg. Chem.* **2007**, *46*, 3367.
(21) Gennari, M.; Lanfranchi, M.; Marchiò, L. *Inorg. Chim. Acta* **2009**, *362*, 4430.
(22) Gennari, M.; Tegoni, M.; Lanfranchi, M.; Pellinghelli, M. A.; Giannetto, M.; Marchiò, L. *Inorg. Chem.* **2008**, *47*, 2223.
(23) Higgs, T. C.; Ji, D.; Czernuszewicz, R. S.; Matzanke, B. F.; Schunemann, V.; Trautwein, A. X.; Helliwell, M.; Ramirez, W.; Carrano, C. J. *Inorg. Chem.* **1998**, *37*, 2383.
(24) The, K. I.; Peterson, L. K.; Kiehlmann, E. *Can. J. Chem.* **1973**, *51*, 2448.
(25) Gennari, M.; Bassanetti, I.; Marchiò, L. *Polyhedron* **2010**, *29*, 361.
(26) The octanol-water partition coefficient P is the common quantitative descriptor of lipophilicity. P is defined as the ratio of the concentrations of a compound in two immiscible phases (octanol and water) under equilibrium conditions. It is mostly used in its logarithmic form, logP. Experimental procedures to measure logP are described in detail in: Sangster, J. *Octanol-water partition coefficients: Fundamentals and physical chemistry*; John Wiley & Sons Ltd.: Chichester, 1997. In the present work, the calculation of the logP values was performed with fragmental methods implemented in the ALOGPS program:*VCCLAB*, Virtual Computational Chemistry Laboratory; http://www.vcclab.org, 2005.
(27) Gozzelino, R.; Jeney, V.; Soares, M. P. *Annu. Rev. Pharmacol. Toxicol.* **2010**, *50*, 323.
(28) Zhang, H. J.; Chen, D.; Ringler, J.; Chen, W.; Cui, Q. C.; Ethier, S. P.; Dou, Q. P.; Wu, G. J. *Cancer Res.* **2010**, *70*, 3996.
(29) Iljin, K.; Ketola, K.; Vainio, P.; Halonen, P.; Kohonen, P.; Fey, V.; Grafstrom, R. C.; Perala, M.; Kallioniemi, O. *Clin. Cancer Res.* **2009**, *15*, 6070.
(30) Zhai, S. M.; Yang, L.; Cui, Q. C.; Sun, Y.; Dou, Q. P.; Yan, B. *J. Biol. Inorg. Chem.* **2010**, *15*, 259.
(31) Chen, D.; Cui, Q. Z. C.; Yang, H. J.; Dou, Q. P. *Cancer Res.* **2006**, *66*, 10425.
(32) Cen, D. Z.; Brayton, D.; Shahandeh, B.; Meyskens, F. L.; Farmer, P. J. *J. Med. Chem.* **2004**, *47*, 6914.
(33) Kar, R.; Singha, P. K.; Venkatachalam, M. A.; Saikumar, P. *Oncogene* **2009**, *28*, 2556.
(34) Szegezdi, E.; Logue, S. E.; Gorman, A. M.; Samali, A. *Embo Rep.* **2006**, *7*, 880.
(35) Rae, T. D.; Schmidt, P. J.; Pufahl, R. A.; Culotta, V. C.; O'Halloran, T. V. *Science* **1999**, *284*, 805.
(36) Valko, M.; Rhodes, C. J.; Moncol, J.; Izakovic, M.; Mazur, M. *Chem. Biol. Inter.* **2006**, *160*, 1.
(37) Tardito, S.; Bussolati, O.; Maffini, M.; Tegoni, M.; Giannetto, M.; Dall'Asta, V.; Franchi-Gazzola, R.; Lanfranchi, M.; Pellinghelli, M. A.; Mucchino, C.; Mori, G.; Marchiò, L. *J. Med. Chem.* **2007**, *50*, 1916.
(38) Malhotra, J. D.; Kaufman, R. J. *Antioxid. Redox Signal* **2007**, *9*, 2277.
(39) Daniel, K. G.; Chen, D.; Yan, B.; Dou, Q. P. *Front. Biosci.* **2007**, *12*, 135.
(40) Perry, D. K.; Smyth, M. J.; Stennicke, H. R.; Salvesen, G. S.; Duriez, P.; Poirier, G. G.; Hannun, Y. A. *J. Biol. Chem.* **1997**, *272*, 18530.